

Redox active PTM radical dendrimers as promising multifunctional molecular switches.

Vega Lloveras, Flonja Liko, Jose L. Muñoz-Gómez, Jaume Veciana, and José Vidal-Gancedo

Chem. Mater., **Just Accepted Manuscript** • DOI: 10.1021/acs.chemmater.9b03015 • Publication Date (Web): 31 Oct 2019

Downloaded from pubs.acs.org on November 3, 2019

Just Accepted

“Just Accepted” manuscripts have been peer-reviewed and accepted for publication. They are posted online prior to technical editing, formatting for publication and author proofing. The American Chemical Society provides “Just Accepted” as a service to the research community to expedite the dissemination of scientific material as soon as possible after acceptance. “Just Accepted” manuscripts appear in full in PDF format accompanied by an HTML abstract. “Just Accepted” manuscripts have been fully peer reviewed, but should not be considered the official version of record. They are citable by the Digital Object Identifier (DOI®). “Just Accepted” is an optional service offered to authors. Therefore, the “Just Accepted” Web site may not include all articles that will be published in the journal. After a manuscript is technically edited and formatted, it will be removed from the “Just Accepted” Web site and published as an ASAP article. Note that technical editing may introduce minor changes to the manuscript text and/or graphics which could affect content, and all legal disclaimers and ethical guidelines that apply to the journal pertain. ACS cannot be held responsible for errors or consequences arising from the use of information contained in these “Just Accepted” manuscripts.

1
2
3
4
5
6 **Redox active PTM radical dendrimers as promising multifunctional**
7 **molecular switches.**
8
9

10 Vega Lloveras,[a],[b] Flonja Liko,[a] José L. Muñoz-Gómez,[a] Jaume Veciana,[a],[b] and José
11 Vidal-Gancedo*[a],[b]
12

13 [a] Institut de Ciència de Materials de Barcelona (ICMAB-CSIC), Campus universitari de Bellaterra, E-08193,
14 Cerdanyola del Vallès (Spain)

15 E-mail: j.vidal@icmab.es

16 [b] Networking Research Center on Bioengineering, Biomaterials and Nanomedicine (CIBER-BBN), Barcelona
17 (Spain).
18
19
20

21 *Supporting Information Placeholder*
22
23
24
25
26
27
28
29
30
31
32
33
34
35
36
37
38
39
40
41
42
43
44
45
46
47
48
49
50
51
52
53
54
55
56
57
58
59
60

ABSTRACT: Nowadays there is a great interest in using individual molecules as nanometer-scale switches and logic devices, with the aim of reaching higher power and smaller size. Demonstrating that one molecular switch can be turned on and off in room temperature, simply by applying a current to a neighboring molecule has interesting implications. Herein we report the synthesis, characterization and behavior of three generations of polyphosphorhydrazone (PPH) dendrimers, fully functionalized with 6, 12 and 24 redox active perchlorotriphenylmethyl (PTM) radicals in the periphery, capable of undergoing an electrochemical reversible switching by multi-electron reduction and oxidation. An electrical input was used to trigger the physical properties of these radical dendrimers in a reversible way, modifying their optical, magnetic and electronic properties. Our $G_n(\text{PTM}^*)_x$ radical dendrimers are paramagnetic, exhibit an absorbance band at 386 nm and red fluorescence emission, if in radical state. When they are switched to their anion state, these dendrimers convert to diamagnetic species with a maximum absorbance band at ca. 520 nm and no fluorescence emission. Due to two different molecular states, the switch undergoes a reversible and important color change, from light brown for $G_0(\text{PTM}^*)_6$ and bright yellow for $G_1(\text{PTM}^*)_{12}$ and $G_2(\text{PTM}^*)_{24}$ dendrimers, when in radical state, to either deep wine color for $G_0(\text{PTM}^-)_6$ or purple colors for $G_1(\text{PTM}^-)_{12}$ and $G_2(\text{PTM}^-)_{24}$ dendrimers, when in the anion state. Furthermore, there exists a viable opportunity to control the exact number of electrons transferred during the switching process, that could lead not only to a two-state but also to a multi-state switch in the near future. This is the first molecular switch based on organic radical dendrimers, in our best knowledge. Moreover, these species can act as electron accumulative molecules able to accept and release up to 24 electrons per molecule at very accessible potentials and in a reversible way.

INTRODUCTION

The miniaturization of future technologies is a current hot topic, aiming to design multi-responsive molecular systems. The successful development of an innovative molecular switch requires integrating successfully several switchable functions into a single macromolecular architecture. Conventional molecular switches include photochromic switches,¹ fluorescence switches,² chiral switches,³ redox switches,⁴ and pH switches⁵. Dendrimers are especially appealing globular macromolecules characterized by a controlled synthesis that suits well the preparation of monodisperse nanosystems with tunable size and precise number of peripheral groups.⁶ The multivalency attribute of the dendrimers is useful to synthesize many multifunctional nanosystems^{7,8} either with synergistically integrated drugs,^{9,10} radiotherapeutics,¹¹ or functional radicals,^{12-16,17} and diverse probes.^{18,19} Dendrimers allow a perfect location of functional groups, what makes them a powerful tool for fine studies of electron-transfer kinetic and thermodynamic parameters in biosystems and materials science. Electron-transfer processes in molecular assemblies on the nanoscale level have served to prepare supramolecular

redox sensors and surface modified electrodes and are also of crucial importance for many fundamental biological processes.²⁰ An increasing number of dendrimers have been functionalized with stable redox active pendant groups, such as tetrathiafulvalene and ferrocene, aiming at materials with a wide variety of functional properties.²¹⁻²³ In these cases, multi-electron oxidations to the corresponding cations could be accomplished. The use of electroactive organic radicals as molecular switches offers new opportunities, since they are allowed to electrochemically trigger not only the optical but also other physical responses, such as magnetism. It is of prime importance to have a secondary physical signal, in order to be able to read the state of the switch non-destructively. In our best knowledge, this is the first example of a stimuli-responsive molecular switch based on radical dendrimers, in which an electrical input is transduced into both optical and magnetic outputs that can be employed as read-out mechanisms, to achieve perspective molecular machines or read/write memory devices (Figure 1). Other important property of radical dendrimers is the possibility to act as electron accumulative molecules. Molecules that can store a high number of electrons find important and wide applications for the design of multiple devices in molecular electronics. These applications are generally based on good electron accepting properties along with no decomposition or change in their structural arrangement. Some examples are C_{60} ,²⁴ polyoxometallates (POMs)²⁵, metallocarborane compounds²⁶ or metal dendrimers.²⁷

Magnetic interactions between neighboring radicals, not only in radical dendrimers, but also in radical polymers, gold nanoparticles or other supramolecular species, could determine the most important properties of these compounds in different applications.²⁸⁻³¹ Members of the family of PTM radicals are chemically and thermally persistent due to the fact that their open-shell centers are shielded by six bulky chlorine atoms. In addition, they are bistable in terms of their electroactive character, as they can be easily and reversibly reduced to the carboanion form.³² Because this redox process occurs at very low potentials, these molecules are promising for applications in charge storage memory devices. The redox pair also demonstrates completely different magnetic and optical properties. The PTM radical is a paramagnetic species with maximum absorbance centered at 386 nm and fluorescence emission at 688 nm, but the anion is diamagnetic, with a maximum absorbance at 515 nm, and does not emit fluorescence. In the present work, it is described the synthesis and characterization of three generations of polyphosphorhydrazone (PPH) based dendrimers (G_n , $n=0-2$) fully coupled with PTM radicals in the periphery (6, 12 and 24 PTM radicals, respectively) ($G_n(\text{PTM}^*)_x$, $n=0-2$, $x=6-24$) and their redox-stimulated switching behavior, for potential applications as multifunctional molecular switches. PPH dendrimers were the chosen scaffold, because they could be synthesized as a complete series of generations with high uniformity and because of their terminal aldehyde groups, which could be used to couple radical units with a great variety of linkers. PTM radicals were selected, not only for their remarkable properties, but also since in our best knowledge, the magnetic properties of these radicals coupled to dendrimers, have not yet been studied.

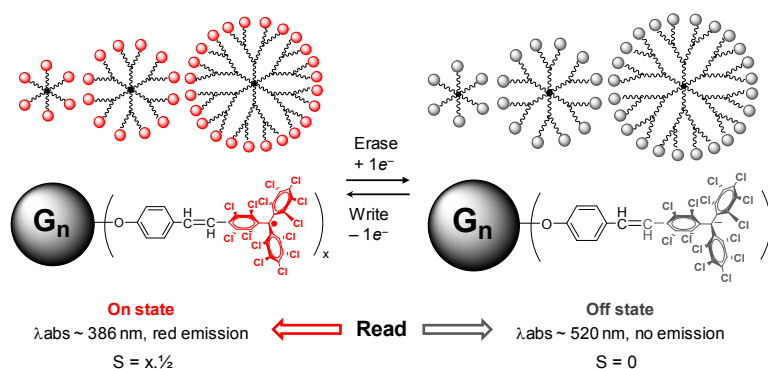


Figure 1. Representation of the electrochemical bistability of PTM radical dendrimers ($G_n(\text{PTM}^\bullet)_x$, $n=0-2$, $x=6-24$). The PTM molecule has two redox states, the radical (left) and anion (right) forms, which can be electrochemically interconverted. Each state exhibits different magnetic and optical properties: radical dendrimers $G_n(\text{PTM}^\bullet)_x$ exhibit spin $S=x/2$, an absorbance band at 386 nm and red fluorescence emission, and anion $G_n(\text{PTM}^-)_x$ is a diamagnetic species with $S=0$, a maximum absorbance band at 516, 518 and 526 nm for $G_n(\text{PTM}^-)_x$ ($n=0-2$, $x=6-24$) radical dendrimers respectively, and is not fluorescent.

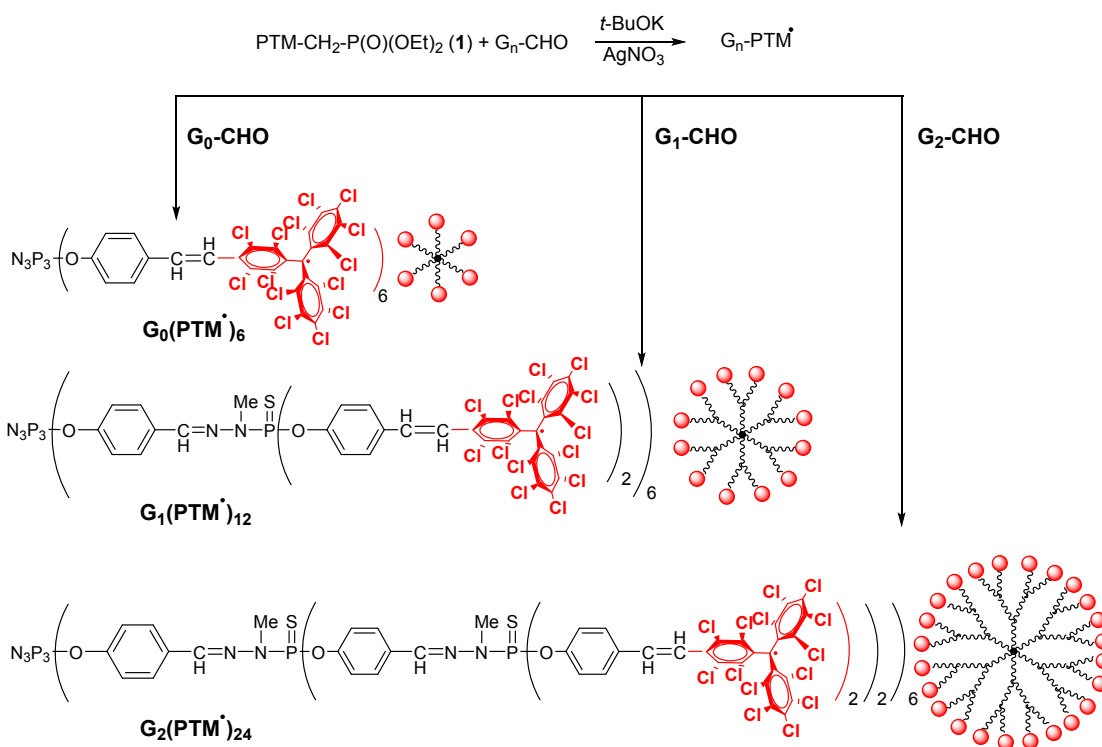
RESULTS AND DISCUSSION

We synthesized three generations of phosphorous containing dendrimers ended in aldehyde groups PPH- G'_n dendrimers ($n = 0, 1, 2$) under the conditions described in literature³³ but with some modifications to improve the reaction yields (see Tables S1-S5 and text in the Supplementary Information). On the other hand, a derivative of PTM radical with a phosphonate group (**1**, Scheme 1) was also prepared according to previously reported procedures,³⁴ (see Scheme S1 in the SI) in order to allow the coupling with the terminal aldehyde groups of the PPH dendrimers using the Wittig-Horner-Emmons reaction.^{34,35} This coupling involved the formation of a double bond between the carbon atom of the aldehyde group and that of the phosphonate derivative, resulting in vinylenes. The conformation of the $-\text{HC}=\text{CH}-$ double bonds formed in Wittig reactions with PTM-phosphonate has always given the *E* conformation³⁶⁻³⁹, as in our radical dendrimers (see Figure S1 and explanation in the SI) because PTM is an electron-withdrawing and bulky substituent and we use potassium *tert*-butoxide as a base.

PTM radical dendrimers (Scheme 1) were synthesized in a one pot reaction. This procedure was similar for all the three generations. An excess of PTM derivative **1** and potassium *tert*-butoxide were dissolved in THF, resulting in a purple colored mixture. This mixture was stirred for 10 minutes to form the phosphonium salt. Afterwards, a solution of the aldehyde terminated G'_n dendrimers ($n = 0, 1, 2$) in THF (1 eq.) was added. The reaction was followed up by IR by the disappearance of the

aldehyde signal at 1700 cm^{-1} and by NMR. Once the reaction was completed, the PTM anions were oxidized to PTM radicals, with an excess of silver nitrate (AgNO_3) in ACN. The conversion of $G_n(\text{PTM}^-)_x$ to $G_n(\text{PTM}^\bullet)_x$ was monitored by UV-Vis with the disappearance of the *ca.* 520 nm band, corresponding to its highest occupied molecular orbital/ lowest energy unoccupied molecular orbital (HOMO-LUMO) transition and the appearance of the band at 386 nm, corresponding to the transition from the singly occupied molecular orbital (SOMO) to LUMO. In all cases, 10-12 minutes of AgNO_3 exposure were enough to get the quantitative formation of the radical. Characterization of the final products was done by phosphorus-31 nuclear magnetic resonance spectroscopy (^{31}P NMR), Fourier transform infrared spectroscopy (FT-IR), matrix assisted laser desorption ionization-time of flight mass spectrometry (MALDI-TOF), size-exclusion chromatography (SEC-GPC), SQUID magnetometry, electron paramagnetic resonance spectroscopy (EPR), cyclic voltammetry (CV) and fluorescence microscopy.

The ^{31}P NMR chemical shifts of the final dendrimers functionalized with PTM radicals (see the Supplementary Information) were not too much affected by the presence of the radicals and presented a shift up to lowest field with respect to the dendrimers ended in aldehyde groups, in agreement with similar modifications described in the literature.^{16,40} Importantly, the shift of ^{31}P NMR signals allowed the monitoring of the reaction and determination of the purity of the new dendrimers confirming that all the branches were substituted.



Scheme 1. Synthetic route of $\text{G}_0(\text{PTM}^\bullet)_6$, $\text{G}_1(\text{PTM}^\bullet)_{12}$, and $\text{G}_2(\text{PTM}^\bullet)_{24}$ radical dendrimers.

By MALDI-TOF it was possible to analyze $\text{G}_n(\text{PTM}^\bullet)_x$ dendrimers of zero and first generation, with 6 and 12 PTM radicals on their periphery, respectively (see the SI). However, it was not possible to analyze with this technique the dendrimer of the second generation $\text{G}_2(\text{PTM}^\bullet)_{24}$, with 24 radicals in its periphery, as it is common for these types of compounds.^{40,41} The purity of the radical dendrimers was verified by SEC-GPC, using CHCl_3 as a solvent (Figure 2).

Quantitative EPR was performed for the three radical dendrimers generations. We observed double EPR signal intensity (measured in terms of area, i.e. double integral of the EPR signal) in the first and second generations with respect to the zero and first generations, respectively, showing, hence, a very good regression coefficient in the regression line of the EPR intensity *versus* the number of radicals plot (see Figure S9).

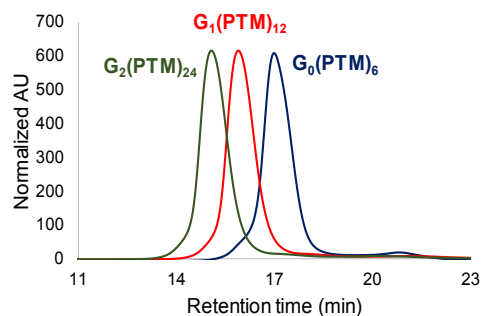
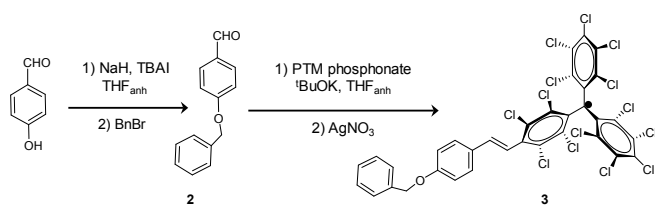


Figure 2. Normalized SEC chromatograms of all three generations of PTM radical dendrimers in CHCl_3 .

The magnetic interactions between radical pendant groups were studied by EPR. Previously, we synthesized a model compound with only one PTM radical unit showing thus no possibility of presenting intramolecular radical-radical interactions. Model compound **3** structurally similar to the terminal part of the dendrimers' branches was synthesized with the aim of studying the changes in the EPR spectra caused by the presence of multiple PTM radicals in the $G_n(\text{PTM}^*)_x$ radical dendrimers compared with it. The first step of the synthesis of compound **3** consisted in the protection of the hydroxyl group of *p*-hydroxybenzaldehyde with benzyl bromide, using NaH as a base and TBAI to afford 4-(benzyloxy)benzaldehyde (**2**) (Scheme 2). The next step was similar to that of the coupling of PTM radicals to PPH dendrimers and consisted of a one pot reaction with two steps. Firstly, the aldehyde group of **2** was reacted with PTM phosphonate **1** in the presence of potassium *tert*-butoxide, subsequently followed by the oxidation with AgNO_3 to the radical. Compound **3** was obtained as a brown solid with a 78% yield and it was characterized by FT-IR, MALDI-TOF and EPR.



Scheme 2. The synthetic route of model compound **3**.

The EPR studies of the three PTM radical dendrimers generations and the model compound **3** were done under isotropic conditions at different temperatures (see Figure 3) as well as under anisotropic conditions (frozen conditions) (see Figure 4).

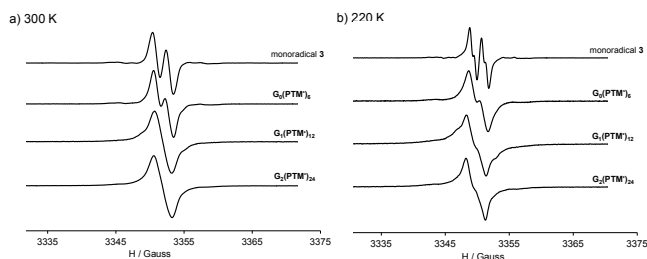


Figure 3. EPR spectra in solution under isotropic conditions of compound **3** and PTM radical dendrimers $G_n(\text{PTM}^*)_x$ ($n=0-2$, $x=6-24$) in dichloromethane:toluene 1:1 at $3.5 \cdot 10^{-4}$ M a) at 300 K and b) at 220 K (the intensities are normalized).

The EPR spectrum of the model compound **3** at 300 K (Figure 3a) showed the two typical lines of a PTM monoradical connected to a $-\text{CH}=\text{CH}-$ double bond, due to the coupling of the unpaired electron with one of the vinylenic H nuclei (a_{H1} , the one farther from the PTM unit), as well as the typical lines due to the coupling with the α and aromatic ^{13}C nuclei of the triphenylmethyl structure (see Table 1 and Figure S10). The EPR spectrum of $G_0(\text{PTM}^*)_6$ was similar to that of **3** (two lines), but with lower resolution (i.e. broader linewidth), due to the dendrimer effect. In this case, the tumbling of the terminal radical units, was slower than that of the free radical, due to the higher molecular size of the dendrimer. Furthermore, the proximity of the terminal radical units in the dendrimer favored the magnetic dipolar-dipolar interactions, resulting also in broader lines. The dendrimer effect increased with the increase in dendrimer generation resulting in overlapped EPR lines, appearing as a one broad center line in the case of $G_1(\text{PTM}^*)_{12}$ and $G_2(\text{PTM}^*)_{24}$ (Figure 3a). For this reason, it was not possible to distinguish the ^1H and ^{13}C coupling constants in these generations. All the EPR data from **3**, $G_0(\text{PTM}^*)_6$, $G_1(\text{PTM}^*)_{12}$, and $G_2(\text{PTM}^*)_{24}$ are summarized in Table 1. All compounds presented a similar g factor, very close to that observed for other PTM radicals.⁴²

Table 1 EPR data of the monoradical **3** and radical dendrimers $G_n(\text{PTM}^*)_x$ ($n=0-2$, $x=6-24$) at 300 K in dichloromethane:toluene 1:1.

Compound	g	a_{H1} (G)	a_{Cu} (G)	a_{Carom} (G)	ΔH_{pp} (G)	ΔH_{sp}^a (G)
3	2.0031	1.9	29.3	12.5; 10.2	1.0	3.1
$G_0(\text{PTM}^*)_6$	2.0035	1.8	29.1	12.4; 10.1	1.2	2.9
$G_1(\text{PTM}^*)_{12}$	2.0035	<i>b</i>	~ 29	~ 12 ; 10	<i>b</i>	2.7
$G_2(\text{PTM}^*)_{24}$	2.0034	<i>b</i>	~ 29	~ 12 ; 10	<i>b</i>	2.7

[a] Total EPR spectrum width. [b] Not distinguishable.

When the temperature decreases, the EPR spectra line width decreases as well. For this reason, when the temperature was decreased to 220 K (Figure 3b), we could observe in monoradical **3** the coupling with the other vinylenic H (a_{H2} , the one closest to the PTM unit), with lower coupling constant ($a_{\text{H2}} = 0.65$ G), showing, only in this case, a four-line spectrum.

In these conditions, the radical dendrimers of higher generations presented a spectral pattern dominated by not well resolved two lines ($a_{H1} \sim 1.8$ G).

Under frozen conditions (120 K) the EPR spectrum of monoradical **3** (Figure 4a) appeared to be quite symmetrical, as occurs in some highly chlorinated triphenylmethyl radicals,⁴² indicating that the anisotropy is low. Under these conditions, the spectra corresponding to the radical dendrimers also presented similar shape; i.e., an intense broad line (Figure 4a) although with lower total width when the generation increases due to the higher radical interactions.¹⁶ However, they also presented additional low intensity quasi symmetrical features (Figure 4b). In the dendrimer conformation, some of the radical units at the end of the branches are expected to be far among them, i.e. not interacting, and other close enough to interact. The contribution of the non-interacting PTM units could lead, in part, to this central broad and intense line as in the monoradical species while the weak satellite lines, only appearing in the radical dendrimers, are due to the dipolar magnetic interactions among radicals, which are indicative of the presence of pairs of closer PTM radical units inside of dendrimers. Such dipolar coupling lines were observed in all radical dendrimers at ca. 3250, 3307, 3328, 3378, 3402, and 3456 Gauss (lines labeled with \diamond and * in Figure 4b). The lines marked with a rhombus could correspond to the magnetic transitions of the closer pairs of radical units produced by dipolar magnetic interactions between two unpaired electrons. From the simulation of such lines (Figure 6), we obtained the zero-field splitting (zfs) parameters, D and E , for each generation, that were similar among them: D values between 50.7 and 51.5 G and $E = 0$, corresponding with an axial symmetry. From the zero-field splitting parameter D it is possible to calculate the average separation between two interacting radical species (R) in a given compound, using the following equation^{43,44} $R^3 = 27887/D$, being R in Å and D in Gauss. An average interspin distance of 8.1-8.2 Å was found for the PTM radical dendrimers. It is worth mentioning that this interspin distance is the same than the obtained from the X-ray diffraction structure of another similar radical dendrimer synthesized by us. In fact, the distance between the interacting radical units in such a radical dendrimer (the zero generation of PPH dendrimer ended in iminoTEMPO groups),¹⁵ was between 7.71 Å and 8.45 Å. The magnetic transitions, marked with * in Figure 4, observed at 3250 and 3456 G with very low intensity together with two other transitions overlapped inside the ones at ca. 3307 and 3402 G and a central one overlapped inside the principal line (see Figures 5 and S10) could correspond to transitions originated by the dipolar interactions of groups of three close PTM radical units in the dendrimers. From the simulation of such lines (Figure 6), we obtained the same zfs parameters (D values ca. 51 G and $E = 0$) for all radical dendrimers. Here it is important to take into account the characteristic conformation of the zero generation of PPH dendrimers consisting of three branches close together above and below the N_3P_3 ring,¹⁵ as this can explain the dipolar magnetic interactions between three close enough radical units, which can also be maintained in the higher generations. With all this information, we can say that in the EPR frozen spectra of the dendrimers we detected a strong contribution of non-interacting PTM units, as well as weaker contributions of dipolar interactions between, at least, groups of two and three

radical units, with a radical-radical distance around 8 Å. Other contributions of two or three radical units with different D values could exist masked inside the more pronounced principal lines. However, the probability of a magnetic interaction between more than three radical species at the same time should be very low or inexistent.

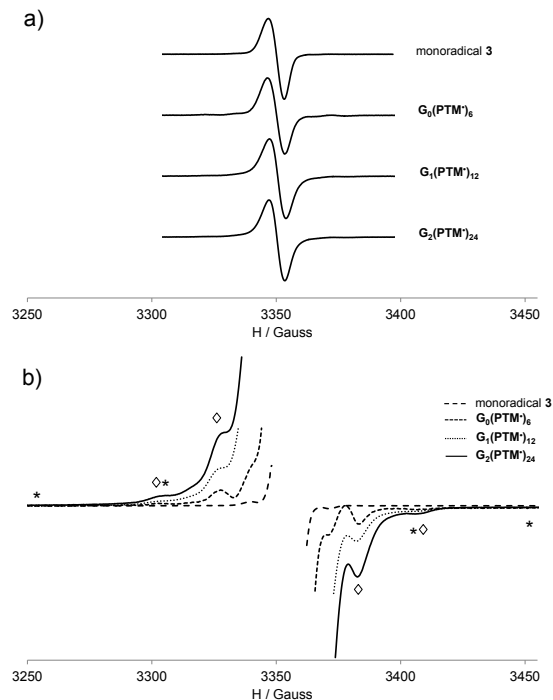


Figure 4. EPR spectra of monoradical **3** and PTM radical dendrimers $G_n(\text{PTM}^*)_x$ ($n=0-2$, $x=6-24$) at 120 K in dichloromethane:toluene 1:1 at $3.5 \cdot 10^{-3}$ M, with normalized intensities. a) Central line. b) Enlarged spectra with the dipolar coupling lines.

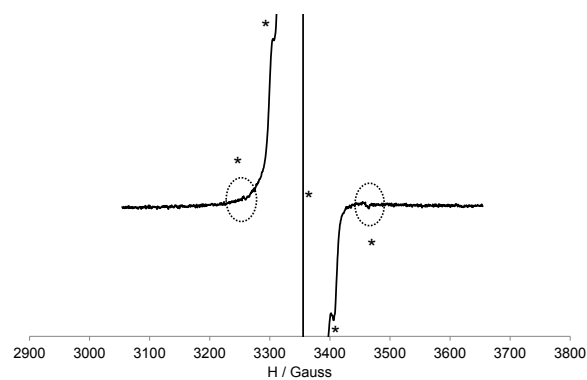


Figure 5. Enlarged EPR spectrum of $G_1(\text{PTM}^*)_{12}$ at 120 K to observe the quartet ($S=3/2$) transitions.

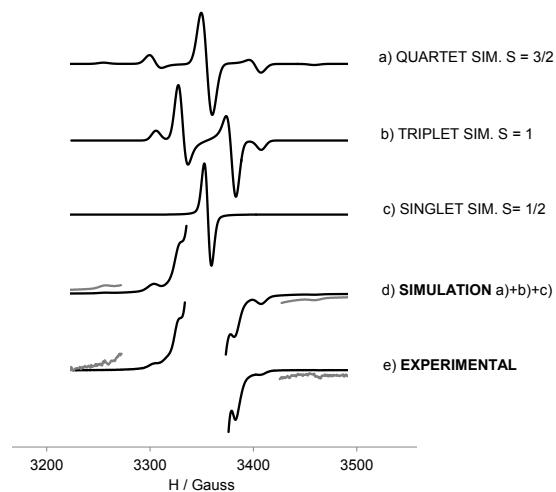


Figure 6. Simulation of the dipolar coupling lines (d) of the experimental EPR spectrum of $G_1(\text{PTM}^*)_{12}$ at 120 K (e). The simulation is the sum of the quartet (a) plus the triplet (b) both with axial symmetry plus the singlet (c). The intensity shown in these simulated spectra (a, b and c) is not the real one used for the sum of the final simulation.

In addition, under such conditions at 120 K, it was also observed in the EPR spectra $|\Delta m_s| = 2$ transitions at half field in all generations (Figure 7), characteristic of dipolar coupled spins. This result gave a direct evidence of the presence of groups of PTM radicals with high-spin ground states or alternatively with low spin ground states but with thermally accessible high spin states in all generations.

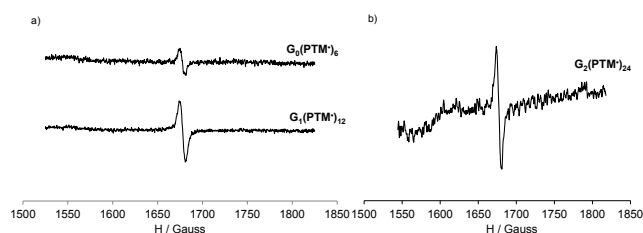


Figure 7. EPR spectra at half field of a) $G_0(\text{PTM}^*)_6$ and $G_1(\text{PTM}^*)_{12}$ at $3.5 \cdot 10^{-3}$ M and b) $G_2(\text{PTM}^*)_{24}$ at $3.5 \cdot 10^{-4}$ M in toluene:DCM 1:1 at 120 K.

Furthermore, the magnetic properties of $G_0(\text{PTM}^*)_6$ and $G_1(\text{PTM}^*)_{12}$ radical dendrimers were investigated by SQUID magnetometry in the temperature range 2–300 K. The corresponding plots of $\chi_M T$ ($\text{cm}^3 \cdot \text{K} \cdot \text{mol}^{-1}$) vs temperature (K) (Figure 8) showed that both compounds follow the Curie-Weiss law with weak antiferromagnetic interactions among PTM radical units at low temperatures (below ca. 40 K). The $\chi_M T$ value of 2.23 and 4.46 $\text{cm}^3 \text{Kmol}^{-1}$ found at 300 K, for the zero and first generations respectively, was very close to the expected contribution of 6 and 12 non-correlated spins (with $S = 6 \cdot \frac{1}{2}$ or $12 \cdot \frac{1}{2}$), for which $\chi_M T$ values of 2.25 and 4.50 $\text{cm}^3 \text{Kmol}^{-1}$, respectively, are theoretically expected. This result confirmed the fully functionalization of all the dendrimers' branches of these dendrimers with pendant PTM radicals.

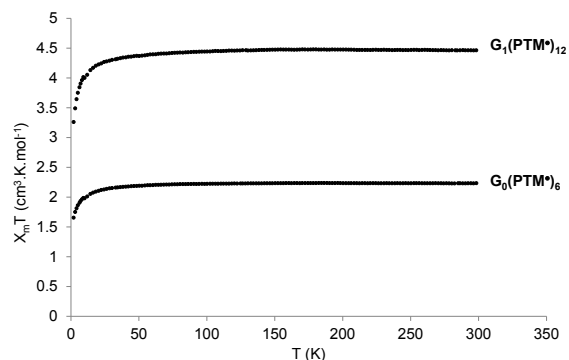


Figure 8. $\chi_M T$ vs T plots for $G_0(\text{PTM}^*)_6$ and $G_1(\text{PTM}^*)_{12}$ radical dendrimers.

Fluorescence microscopy was used to detect fluorescence emission in the radical dendrimers, even in solid state. We observed red fluorescence emission in all the three generations of PTM radical dendrimers $G_0(\text{PTM}^*)_6$, $G_1(\text{PTM}^*)_{12}$ and $G_2(\text{PTM}^*)_{24}$ (Figure 9) when a fluorescence filter with the adequate range of excitation wavelength (330–385 nm) was used. With the other filters we did not observe any emission at all (see Figure S12 as an example).

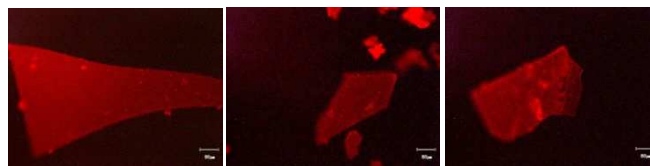


Figure 9. Fluorescence microscopy images showing the red fluorescence of the zero, first and second generation of PTM radical dendrimers compounds (from left to right).

The electrochemical properties of the $G_n(\text{PTM}^*)_x$ ($n=0-2$; $x=6-24$) radical dendrimers were evaluated by cyclic voltammetry⁴⁵ in THF with 0.02 M of tetrabutylammonium hexafluorophosphate (TBAHFP) as electrolyte, using a graphite electrode as the working electrode. Ferrocene was used as an internal standard reference. In Figure 10 we show the voltammograms of $G_0(\text{PTM}^*)_6$, $G_1(\text{PTM}^*)_{12}$ and $G_2(\text{PTM}^*)_{24}$ at different scan rates and the electrochemical data are summarized in Table 2.

Table 2. Experimental data extracted from the voltammograms of $G_n(\text{PTM}^*)_x$ dendrimers. $E_{1/2}^{[a]}$ vs Ag/AgCl.

Compounds	$E_{1/2}$ (V)
3	-0.27
$G_0(\text{PTM}^*)_6$	+0.07
$G_1(\text{PTM}^*)_{12}$	-0.003
$G_2(\text{PTM}^*)_{24}$	-0.04

^[a] $E_{1/2}$ wave potential data taken from the principal E_a and E_c values.

It is worth to remark that the voltammograms of all these dendrimers revealed the presence of one reversible multi-electron reduction process, in spite of well separated sequential redox waves, meaning there exist one reversible process englobing the reduction of 6, 12 and 24 TEMPO units in a small and accessible range of potentials. Although it did not appear different waves, the voltammogram waves of such species were broad and the presence of some shoulders was noticed, that were more pronounced in the higher generations. The presence of these shoulders was an indicator that the reduction process did not occur exactly at the same potential in all the PTM units, probably due to the closer distance between them resulting in higher interactions. In addition to this, we can observe that, by one hand, the average potentials are less negative in the radical dendrimers compared with the monoradical **3** or other PTM monoradicals (typically between -0.2/ -0.3 V vs Ag/AgCl)^{34,46} and, on the other hand, a shift to more negative values with the increase in generation number. All these trends are a clear indication of the mutual interactions between the redox centers existing in these macromolecules and can be explained by means of only intramolecular electronic effects. Thus, cross-conjugation between negative and radical centers would explain the higher stabilization of partially charged species with a large number of radical centers (less negative potentials in radical dendrimers) while intramolecular Coulombic repulsions amongst the existing neighboring anions would

explain the observed increasing destabilization of species with higher negative charges (more negative potentials with the increase in generation).⁴⁷

The potential difference (ΔE , taking into account the principal E_a and E_c peaks) was between 80-120 mV for all generations at a scan rate of 200 mV s⁻¹, an indication of the fast response and high reversibility of the electroactive systems. In addition to this, the peak currents were proportional to the square root of the scan rate in all cases (inset of Figure 10), indicating a reversible electron transfer reaction in terms of the diffusion layer thickness. The stability of the two redox states was confirmed by performing many consecutive voltage cycles, which resulted in identical redox waves without any sign of loss of current intensity. This is an encouraging result indicating the excellent potential of these radical dendrimers to function as reversible and extremely stable molecular switches. In addition, it is important to remark the high electron accepting capacity of such species able to accept up to 24 electrons per molecule in a small range of accessible potentials and in a reversible way. This important characteristic has also been reported in some metal dendrimers by D. Astruc²⁷ and makes them to be good electron accumulative molecules, for the design of other electronic devices.

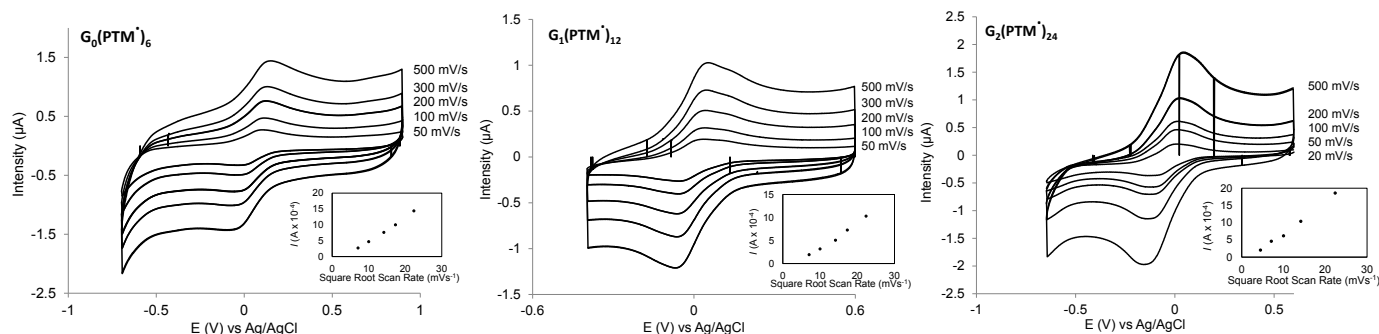


Figure 10. Voltammograms of $G_n(\text{PTM}^*)_x$ ($n=0-2$, $x=6-24$) at different scan rates vs Ag/AgCl in an electrolyte solution of 0.02 M of TBAHFP in THF. Inset: plot of anodic current vs square root of scan rate.

The presence of a secondary physical signal is of crucial importance to read the state of a switch non-destructively in read/write memory devices. To check the response of the switch we used two methods simultaneously. Since the PTM radical has paramagnetic properties ($S=1/2$) and absorbs at $\lambda=386$ nm, and the PTM anion has diamagnetic properties ($S=0$) and absorbs at different wavelength ($\lambda=515$ nm),⁴² the optical absorption responses of the switch (reduction-oxidation process) were monitored by UV-Vis spectroscopy and subsequently the magnetic response by EPR spectroscopy. In addition, we also monitored the change in the fluorescence emission of the radical (red emission) and the anion (no emission) states with a fluorescence microscope by chemical redox (vide infra).

Electrochemical reduction/oxidation was performed using a Pt mesh electrode as the working electrode and a 0.1 M solution of TBAHFP in anhydrous DCM, degassed with argon. Voltage pulses of -0.7 or -0.9 V and +0.15 V (vs Ag/AgCl) were

applied for 300-750 sec, depending on the dendrimer generation, and the samples were monitored by UV-Vis and EPR. Initially, $G_n(\text{PTM}^*)_x$ dendrimers exhibited an absorption band centered at 386 nm, which corresponds to the radical character of PTM units. After the reduction of radical dendrimers by applying a voltage of -0.7 V (vs Ag/AgCl) for $G_0(\text{PTM}^*)_6$ and $G_1(\text{PTM}^*)_12$ and -0.9 V (vs Ag/AgCl) for $G_2(\text{PTM}^*)_24$, the UV-Vis spectrum showed that the characteristic PTM radical absorption band at 386 nm disappeared, while a broad band centered at 516-526 nm, depending on the dendrimer generation, was observed with the formation of PTM⁻ anions. The radical absorption signal was fully recovered after oxidizing again the radical dendrimers applying a voltage of +0.15 V (vs Ag/AgCl). The optical response for five consecutive cycles of the redox-induced switch of $G_n(\text{PTM}^*)_x$ ($n=0-2$, $x=6-24$) is shown in Figures S12-S14. An important color change was observed, from light brown for $G_0(\text{PTM}^*)_6$ and bright yellow color for

$G_1(\text{PTM}^*)_{12}$ and $G_2(\text{PTM}^*)_{24}$ dendrimers, when in radical state, to either deep wine color for $G_0(\text{PTM}^*)_6$ or purple colors for $G_1(\text{PTM}^*)_{12}$ and $G_2(\text{PTM}^*)_{24}$ dendrimers, when in the anion state (see Figure 11 and S15). Such spectroelectrochemical experiments clearly show that the two redox states of the radical dendrimers can be easily identified by naked eye and

from the UV-Vis spectra, as both forms exhibit distinct intense absorption bands, thereby demonstrating that optical readout of the charge storage is viable.

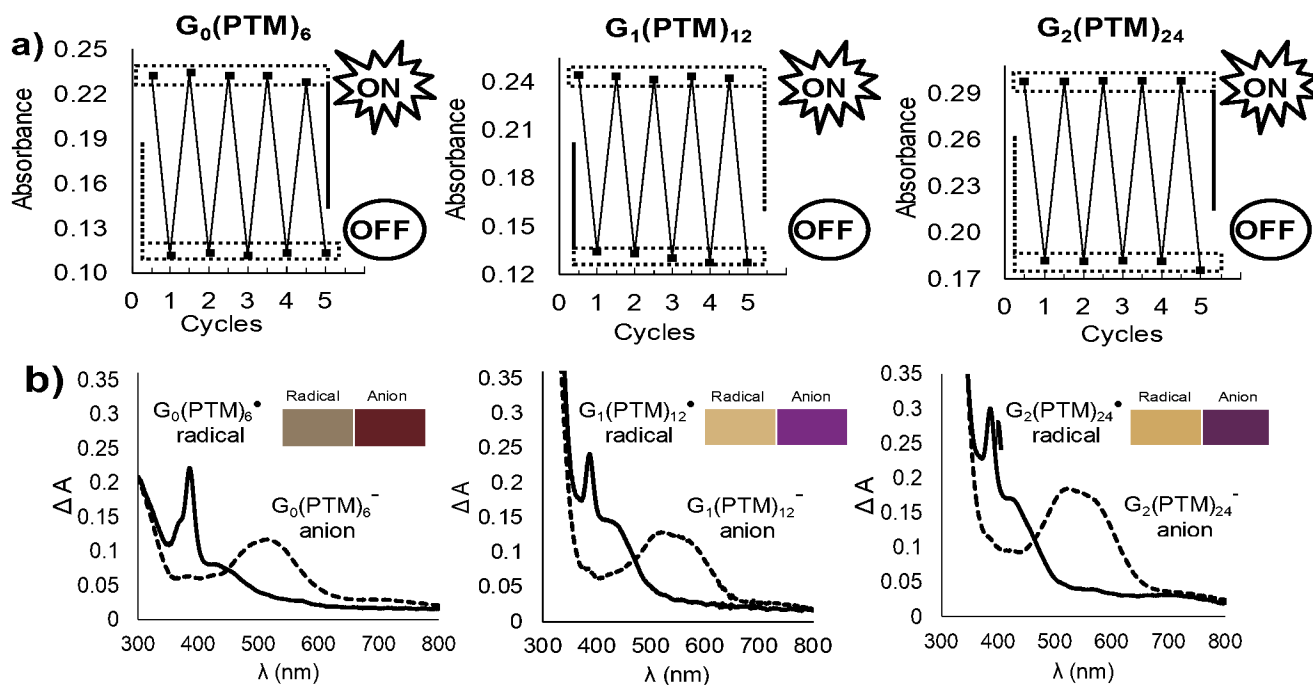


Figure 11. Optical absorption properties of the $G_n(\text{PTM})_x$ ($n=0-2$, $x=6-24$) dendrimers with concentration 0.2-0.4 mM per radical and after in situ electrochemical reduction on applying -0.7 or -0.9 V to the radical and oxidation on application of +0.15 V to the anion state. a) UV-Vis absorption registered during five consecutive cycles, showing the excellent recovery of the absorption values from the ON (radical) to the OFF (anion) states and the high reversibility of the process. b) Illustration of the UV-Vis spectra of the two states of the switch, showing the radical as a solid line and the anion as dashed line. Colorimetric characteristics of both forms are given as an inset and in Figure S16.

Furthermore, taking advantage of the magnetic moment of the organic radical, the magnetic output was simultaneously employed to read the state of the switch. Initially, $G_n(\text{PTM}^*)_x$ radical dendrimers exhibited their corresponding EPR signal, due to the radical character of PTM units. After applying a voltage of -0.7 V (vs Ag/AgCl) for $G_0(\text{PTM}^*)_6$ and $G_1(\text{PTM}^*)_{12}$ and -0.9 V (vs Ag/AgCl) for $G_2(\text{PTM}^*)_{24}$, the EPR signal intensity was very low indicating that the terminal PTM radicals had been reduced to the diamagnetic PTM anions. However, the EPR signal was fully recovered after oxidizing again the radical dendrimers applying a voltage of +0.15 V (vs Ag/AgCl). A sequence of switching cycles could be applied reversibly without showing any sign of deterioration. Figure 12 illustrates the EPR response of one from the five consecutive electrochemical cycles.

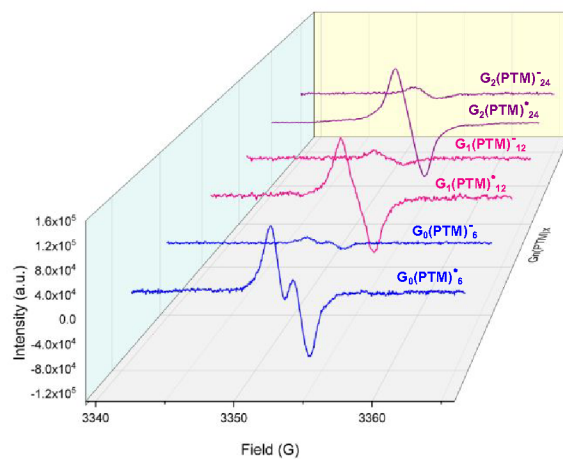


Figure 12. Magnetic responses of the radical dendrimer switch. EPR signal on application of an electrochemical ON/OFF switching cycle of -0.7/-0.9 V for ($G_n(\text{PTM}^*)_x$) and +0.15 V for ($G_n(\text{PTM}^-)_x$) dendrimers. Dendrimers with the PTM in radical state PTM^* corresponds to the ON state and with the PTM in anion state PTM^- to the OFF state.

In addition, to go a step further, it would be very interesting to explore the possibility of controlling quantitatively the reduction (and oxidation) process of the PTM units of the radical dendrimers stepwise. In other words, the number of PTM radicals that undergo redox in the periphery of dendrimers, could be specifically determined and set as demanded in a future application. A preliminary example is shown in Figure 13, where the conversion process from $G_1(\text{PTM}^\bullet)_{12}$ radical to $G_1(\text{PTM}^-)_{12}$ anion is given in four different steps by changing the charge (Q) applied. Such a process was completely reversible. Therefore, by controlling the charge supplied to the system, the redox process could be quantitatively controlled stepwise, opening new perspectives of obtaining not only two-state redox switches but also multi-state redox switches.

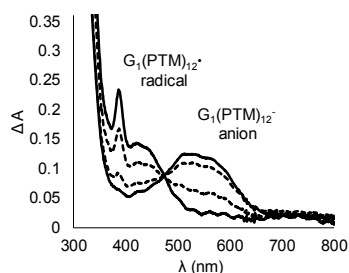


Figure 13. Optical absorption of the conversion process from $G_1(\text{PTM})_{12}^\bullet$ radical to $G_1(\text{PTM})_{12}^-$ anion in different steps.

We also monitored the state of the switch by reading its fluorescence output with a fluorescence microscope, since the radical units present red emission and the anions do not. We controlled the switch chemically by using DBU as reducing agent and AgNO_3 as oxidizing agent. To show the viability of such a switch we performed it with the zero generation radical dendrimer. Initially, some drops of a DCM solution of $G_0(\text{PTM}^\bullet)_6$ radical dendrimer were deposited in a porta and once the solvent was evaporated we observed red emission in the optical microscope using the adequate filter (excitation wavelength range 330–385 nm). Then, we added some drops of DBU base and the color changed immediately from brownish to deep wine (see Figure S17). After letting the solvent evaporate we observed no fluorescence emission with the same filter. However, the red fluorescence emission was recovered again after the addition of some drops of AgNO_3 in CH_3CN solution (Figure 14). This study also demonstrates that the switch can also be controlled chemically.

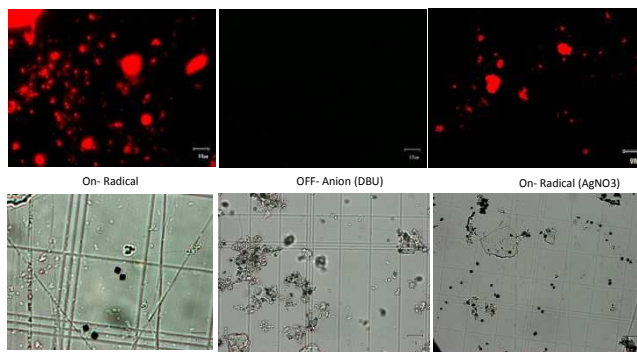


Figure 14. Fluorescence microscope images of the chemical switch of $G_0(\text{PTM}^\bullet)_6$ radical dendrimer.

Conclusions

Three generations of PPH dendrimers, fully decorated in its periphery with 6, 12 and 24 terminal PTM radicals, were synthesized and fully characterized. An extensive EPR study of such radical dendrimers have been accomplished demonstrating that in these systems most of the PTM radicals units inside the dendrimers are non-interacting magnetically although few of them are close enough to interact in pairs or triads. The redox activity of PTM radicals that are easily reduced to their corresponding carbanion has been exploited to fabricate electrochemical switches with optical (absorption and fluorescence) and magnetic responses. A combinational logic function can be implemented with such molecular switches able to transduce two chemical or electrochemical inputs into optical and magnetic outputs. Moreover, in this work we open the perspective of controlling such a switch stepwise to obtain multi-state redox switches. In addition, the high electron accepting capacity of these radical dendrimers able to accept and donate 6, 12 or 24 electrons per molecule at the same time at very accessible potentials and in a reversible way make them to be good electron accumulative molecules. Undoubtedly, the high control over the synthesis, stability and reversibility of systems like the ones reported here, further supports the perspective of using macromolecules as scaffolds in the electronic devices of the future.

Experimental Section

Materials and Methods

All reactions were carried out in inert atmosphere conditions and under constant magnetic stirring. Anhydrous solvents were used. The temperature of the reflux reaction was set to 65°C, if not otherwise specified. Synthesis of the model monoradical **3** and the radical dendrimers was done with a Schenk flask.

Size exclusion chromatography (SEC-GPC) analysis was carried out using an Agilent 1260 infinity II HPLC System apparatus equipped with a diode array detector under the following conditions. For all the three generations of PTM radical dendrimers PSS SDV pre-column (3 μm , 8 x 50 mm) and a PSS SDV analytical column (3 μm , 1000 Å, 8 x 300 mm) with a diode array detector (280 nm) was used. CHCl_3 was used as eluent at a flow rate of 0.5 mL/min at 35 °C. Dendrimers were dissolved in the eluent to reach a final concentration of 1 mg/mL before filtration. Afterwards the solutions were filtered through 0.2 μm before injection.

EPR spectra were obtained with an X-Band Bruker ELEXYS 500 spectrometer equipped with a TE102 microwave cavity, a Bruker variable temperature unit, a field frequency lock system Bruker ER 033 M and equipped with a NMR Gaussmeter Bruker ER 035 M. The modulation amplitude was kept well below the line width, and the microwave power was well below saturation. All samples were previously degassed with Ar. **Magnetic measurements** down to 2 K were carried out in a Quantum Design MPMS-5S SQUID magnetometer. The molar susceptibility was corrected for the sample holder and for the diamagnetic contribution of all atoms by means of Pascal's tables. The diamagnetism of a molecule could be determined in an additive way using the values for the diamagnetic susceptibility of every atom and bond in the molecule.

IR spectra were recorded in the attenuated total reflectance mode (ATR) in a Perkin Elmer Spectrum One Fourier transform spectrometer, with a scan range from 4000 cm^{-1} to 650 cm^{-1} .

The CV measurements were done with a potentiostat Autolab/PGSTAT204 Metrohm in a standard 3 electrodes cell. For the electrochemical characterization studies $G_n(\text{PTM}^*)_x$ radical dendrimers were dissolved in 0.02 M of TBAHFP in THF as electrolyte and using a graphite electrode as the working electrode, a Ag/AgCl reference electrode and a platinum wire as the auxiliary electrode. Ferrocene was used as an internal standard reference. The CVs were carried out at different scan rates. For the switching experiments the same potentiostat was used, however 0.1 M TBAHFP in anhydrous DCM was used as electrolyte and a mesh platinum electrode was used as the working electrode, a Ag/AgCl electrode as the reference electrode and a platinum wire as the auxiliary electrode. The concentrations of dendrimers varied from 0.2-0.4 mM per radical.

UV-Vis spectra were recorded in a double beam UV-Vis-NIR CARY 5 spectrophotometer with a scan range of 250-800 nm.

NMR spectra were recorded with a Bruker AC250 instrument. ^1H NMR (250 MHz, CDCl_3) and ^{31}P NMR (100 MHz, CDCl_3).

Fluorescence Microscopy images were obtained using an Olympus BX51 microscope equipped with different fluorescence filters: U-MWUS3 excitation range λ 330-385 nm and emission from 420 nm up, U-MWBS3 excitation range λ 450-480 nm and emission from 515 nm up and U-MWGS3 excitation range λ 510-550 nm and emission from 590 nm up. Only by using the U-MWUS3 filter we could observe the red fluorescence in the radical dendrimers.

- Synthesis and characterization of three generations of PPH-CHO G_n ' dendrimers

The synthesis of PPH dendrimers ended in -CHO (G_0 , G_1 ' and G_2 ') was performed following the procedure already described in the literature,³³ but with some modifications to improve the reaction yields (see the SI).

- Synthesis and characterization of the PTM phosphonate (1).

The synthesis of diethyl-4-[bis(2,3,4,5,6-pentachlorophenyl)methyl]-2,3,5,6-tetrachlorobenzyl phosphonate was performed following the procedure already described in the literature (see Scheme S1 and text in the SI).³⁴

For the ^1H NMR spectra assignment see the H labels in the SI.

Synthesis of 4-Methyltriphenylcarbinol (1a). 3.2 g (130.7 mmol, 1.1 eq) of magnesium and 0.1 g (0.8 mmol) of iodine were suspended in anhydrous diethyl ether under argon atmosphere at reflux temperature. A solution of 20.0 g (116.95 mmol, 1 eq) of *p*-bromotoluene in 45 mL of diethyl ether was slowly added and constantly stirred for 30 minutes. After 2 hours, a solution of 20.8 g (114.2 mmol, 0.98 eq) of benzophenone in 100 mL of diethyl ether was added drop by drop to the reaction mixture and it was refluxed for 1 hour. The reddish solution was constantly stirred for 18 hours. Then, the reaction mixture was poured over an ice bath (50 g of ice) previously acidified with 2.5 mL of sulfuric acid 2 M, and it was extracted with diethyl ether. The organic phase was washed with sodium bicarbonate (5% p/v) and water. Then, it was dried over anhydrous magnesium sulfate and filtrated. The solvent was eliminated under vacuum. The yellow solid obtained was crystallized with a mixture of hexane and dichloromethane (3/1) and the desired compound was obtained (13 g, 41%). ^1H NMR (250 MHz, CDCl_3): δ 2.35 (s, 3H, Ha),

2.75 (s, 1H, Hb), 7.1-7.3 (m, 14H, HAr) ppm. MS (MALDI-TOF, negative mode): m/z 274 [M-H]⁻. Calculated: $\text{C}_{20}\text{H}_{18}\text{O}$: 274.4.

4-Methyltriphenylmethane (1b). 13 g (47.4 mmol, 1 eq) of 4-methyltriphenylcarbinol (**1a**) were refluxed in 140 mL (364 mmol) of formic acid under argon atmosphere with constant stirring for 24 hours. The reaction mixture changed from dark green to pale pink. After this time, the mixture was cooled down to room temperature and 100 mL of water were added. The mixture was stirred for 30 minutes. Progressively, a white solid started to precipitate. It was dissolved with diethyl ether and a solution of saturated sodium bicarbonate was added until the aqueous solution was neutralized. Then, the organic phase was dried over anhydrous magnesium sulfate, filtrated, and the solvent removed under vacuum. The white powder obtained was purified by column chromatography on silica gel with mixtures of hexane and dichloromethane as eluent. A white powder (11 g, 90%) of the desired compound was obtained. ^1H NMR (250 MHz, CDCl_3): δ 2.3 (s, 3H, Ha), 5.5 (s, 1H, Hb), 7.0-7.3 (m, 14H, HAr) ppm. MS (MALDI-TOF, negative mode): m/z 257 [M-H]⁻. Calculated: $\text{C}_{20}\text{H}_{18}$: 258.4.

α H-tetradecachloro-4-methyltriphenylmethane (1c). 3.85 g (28.6 mmol, 0.37 eq) of AlCl_3 , 4.5 mL of SO_2Cl_2 (56 mmol, 0.72 eq) and 850 mL of SO_2Cl_2 were suspended under argon atmosphere. The orange suspension was refluxed under stirring and 20 g (77.4 mmol, 1 eq) of 4-methyltriphenylmethane (**1b**) solved in 400 mL of SO_2Cl_2 were added drop by drop, obtaining a brown reaction mixture. The mixture was refluxed (65 °C) for 10 hours. During this time, small quantities of SO_2Cl_2 were added in order to keep the volume of the reaction mixture constant. After that, the solution was cooled down to room temperature and concentrated in vacuum to half the volume. The mixture was poured over an ice bath (400 mL) and it was neutralized after slow additions of sodium bicarbonate until the obtaining of pH 7. The mixture was heated to 60 °C and the mixture was acidified with HCl until pH 2.5, obtaining a green precipitate. This solid was dissolved in CHCl_3 and washed with water. Finally, the organic phase was dried over anhydrous magnesium sulfate, filtrated, and the solvent eliminated under vacuum. The green solid was purified by digestion with refluxing pentane. The white solid was filtered under vacuum obtaining 40 g (70%) of the desired product. ^1H NMR (250 MHz, CDCl_3): δ 2.63 (s, 3H, Ha), 6.99 (s, 1H, Hb) ppm. MS (MALDI-TOF, negative mode): m/z 738 [M-H]⁻. Calculated: $\text{C}_{20}\text{H}_4\text{Cl}_{14}$: 740.6. The spectrum shows a broad band due to the isotopic abundance of chlorine (^{35}Cl 76% and ^{37}Cl 24%).

α H-(4-bromomethyl)tetradecachloromethyltriphenylmethane (1d). 14 g (17 mmol, 1 eq) of α H-tetradecachloro-4-methyltriphenylmethane (**1c**) were dissolved in 1.2 L of CCl_4 under argon atmosphere. Then, the solution was heated up to reflux with a white lamp (500 W) and 28 mL (566 mmol, 33.3 eq) of bromine were added. The mixture was refluxed for 6 hours. After this time, the mixture was cooled down to room temperature and the excess of bromine was eliminated by slowly addition of sodium bisulfite. Then, the organic phase was neutralized with sodium bicarbonate until pH 7, extracted with dichloromethane and dried over anhydrous magnesium sulfate. The solvent was removed under vacuum, and the white powder obtained was purified by column chromatography on silica gel with mixtures of hexane and dichloromethane as eluent. The product was obtained as white-brown solid (12.8 g, 83%). ^1H NMR (250 MHz, CDCl_3): δ 4.8 (s, 2H, Ha), 7.0 (s, 1H, Hb) ppm. MS (MALDI-TOF, negative mode): m/z 740 [M-Br]⁻. Calculated: $\text{C}_{20}\text{H}_3\text{BrCl}_{14}$: 819.5. The spectrum shows a broad band due to the isotopic abundance of chlorine.

Synthesis of diethyl 4-[bis(2,3,4,5,6-pentachlorophenyl)methyl]-2,3,5,6-tetrachlorobenzyl phosphonate (1). In a 250 mL flask, 12.0 g (24.4 mmol, 1 eq) of α H-(4-bromomethyl)tetradecachloromethyltriphenylmethane (**1d**) were dissolved in 100 mL (162 mmol) of triethyl phosphite. The mixture was refluxed at 160 °C with anhydrous CaCl_2 tube coupled in the cooling. After three hours it was cooled down to room temperature and 700 mL of water were added. The aqueous phase was extracted with chloroform for 3 times. The combined organic phase was washed with water, dried over anhydrous magnesium sulfate and filtered. The solvent was removed under vacuum. The product was purified by column chromatography on silica gel with mixtures of hexane and ethyl acetate as eluents. The product was isolated as a white powder (10.3 g, 80%). ^{31}P [^1H] NMR (100 MHz, CDCl_3): δ 22 (s, P) ppm. ^1H NMR (250

MHz, CDCl₃): δ 1.3 (*t*, 6H, JHaHb=7.5 Hz, Ha), 3.8 (*d*, 2H, JHcP=22.5 Hz, Hc), 4.1 (*td*, 4H, JHbP=7.5 Hz, JHbHa=7.3 Hz, Hb), 7.0 (*d*, 1H, JHdP=2.5 Hz, Hd) ppm. MS (MALDI-TOF, negative mode): *m/z* 875 [M-H]⁻. Calculated: C₂₄H₁₃Cl₁₄O₃P: 877. The spectrum shows a broad band due to the isotopic abundance of chlorine.

- Synthesis and characterization of the three generations of PTM radical dendrimers

Synthesis of G₀(PTM*)₆: 733 mg of diethyl 4-[bis(2,3,4,5,6-pentachlorophenyl)methyl]-2,3,5,6-tetrachlorobenzyl phosphonate **1** (836 μmol, 7.2 eq) and 188 mg of potassium tert-butoxide (1.67 mmol, 1.4 eq) were dissolved in 2 ml of THF. After 10 minutes stirring, a solution of 0.1 g of G₀-CHO dendrimers (116 μmol, 1 eq) dissolved in 3 ml of THF was added drop-wise with a cannula. The color of the reaction mixture changed from orange to violet. The reaction was monitored by IR-ATR and NMR and it was completed in 18 hours. Afterwards, 158 mg of AgNO₃ (928 μmol, 8 eq) were added and the conversion of the anion into the radical was monitored by UV-Vis. After 5 minutes, an additional 158 mg of AgNO₃ (928 μmol, 8 eq) were added. After the full oxidation of the PTM anion units, the reaction mixture was filtered. Finally, the solvent was removed under vacuum and the product purified by two chromatography columns. The first column was on Bio-Beads™gel (size exclusion chromatography) using THF with HPLC grade as eluent while the second column was on silica gel also using THF with HPLC grade as eluent. The product was isolated as brown-green powder (229 mg, 38%). ³¹P{¹H} NMR (100 MHz, CDCl₃): 9.3 (*s*, P₀) ppm. MS (MALDI-TOF, positive mode): *m/z* 5196 [M+H]⁺. Calculated: C₁₆₂H₃₆Cl₈₄N₃O₆P₃: 5191. The spectrum shows a broad band due to the isotopic abundance of chlorine. IR-ATR (ν/cm⁻¹): 1602, 1504, 1339, 1181, 1159, 1036, 950, 808. EPR (DCM/Toluene 1/1): *g* = 2.0035, *a*_{H1} = 1.8 G, *a*¹³C_α = 29.1 G; *a*¹³C_{arom} = 10.1, 12.4 G; Δ*H*_{pp} = 1.2 G, Δ*H*_{sp} = 2.9 G. CV (0.02 M TBAHFP in THF vs Ag/AgCl): E_{1/2} = +0.07 V (see text). GPC-SEC: Column: PSS SDV analytical column (3 μm, 1000 Å, 8 × 300 mm). Solvent: CHCl₃. λ = 280 nm. 5mL/min, 35°C. Peak at 17.062 min.

Synthesis of G₁(PTM*)₁₂: The synthesis of G₁(PTM*)₁₂ was similar to the G₀(PTM*)₆, but with some modifications in the quantities of the reagents used. 442 mg of **1** (504 μmol, 14.4 eq), and 118 mg of potassium tert-butoxide (1.1 mmol, 31 eq) were dissolved in 2 ml of THF. A solution of 0.1 g G₁-CHO dendrimers (35 μmol, 1 eq) in 3 ml of THF was added drop-wise with a cannula. 94 mg AgNO₃ (560 μmol, 16 eq) were added as oxidant. After 5 minutes, an additional 94 mg AgNO₃ (560 μmol, 16 eq) were added. Following the above described purification procedures the desired product was isolated as a brown-green powder (220 mg, 55%). ³¹P{¹H} NMR (100 MHz, CDCl₃): δ 8.5 (*s*, P₀), 62.7 (*s*, P₁) ppm. MS (MALDI-TOF, positive mode): *m/z* 11537 [M+Na]⁺, and peaks of breakage of 1, 2, 3 and 4 hydrazone bonds (9786, 7990, 6220, 4425). Calculated: C₃₇₂H₁₁₈Cl₁₆₈N₁₅O₁₈P₃S₆: 11512. IR-ATR (ν/cm⁻¹): 1601, 1504, 1337, 1196, 1160, 1040, 941, 817. EPR (DCM/Toluene 1/1): *g* = 2.0035, the line is too broad to determine the hyperfine coupling constant *a*_{H1} and the linewidth; *a*¹³C_α ~ 29 G; *a*¹³C_{arom} ~ 10, 12 G; Δ*H*_{sp} = 2.7 G (see text). CV (0.02 M TBAHFP in THF vs Ag/AgCl): E_{1/2} = -0.003 V (see text). GPC-SEC: Column: PSS SDV analytical column (3 μm, 1000 Å, 8 × 300 mm). Solvent: CHCl₃. λ = 280 nm. 5mL/min, 35°C. Peak at 15.899 min.

Synthesis of G₂(PTM*)₂₄. This synthesis was also similar to the G₀(PTM*)₆. 369 mg of **1** (421 μmol, 28.8 eq) and 94 mg of potassium tert-butoxide (842 μmol, 57.6 eq) were dissolved in 2 ml of THF. A solution of 0.1 g of G₂-CHO dendrimers (14.6 μmol, 1 eq) in 3 ml of THF was added to the reaction mixture drop-wise with a cannula. 75 mg AgNO₃ (438 μmol, 28.8 eq) were added as oxidant. After 5 minutes, an additional 75 mg AgNO₃ (438 μmol, 28.8 eq) were added. Following the above described purification procedures the desired product was isolated as a brown-green powder (141 mg, 40%). IR-ATR (ν/cm⁻¹): 1601, 1504, 1335, 1194, 1162, 1039, 943, 818. EPR (DCM/Toluene 1/1): *g* = 2.0034, the line is too broad to determine the hyperfine coupling constant *a*_{H1} and the linewidth; *a*¹³C_α ~ 29 G; *a*¹³C_{arom} ~ 10, 12 G; Δ*H*_{sp} = 2.7 G (see text). CV (0.02 M TBAHFP in THF vs Ag/AgCl): E_{1/2} = -0.04 V (see text). GPC-

SEC: Column: PSS SDV analytical column (3 μm, 1000 Å, 8 × 300 mm). Solvent: CHCl₃. λ = 280 nm. 5mL/min, 35°C. Peak at 15.078 min.

- **Synthesis and characterization of the PTM model monoradical.** For the ¹H NMR spectra assignment see the H labels in the SI.

Synthesis of 4-(Benzyloxy)benzaldehyde (2). 200 mg of *p*-hydroxybenzaldehyde (1.64 mmol, 1 eq), 55 mg of NaH over mineral oil (2.29 mmol) and 60 mg of TBAI (0.16 mmol, 0.1 eq) were dissolved in 5 ml of THF. 234 μL of benzyl bromide (1.96 mmol, 1.2 eq) were added to the mixture and it was stirred for 18 hours at rt. Afterwards, an aqueous work-up was done (DCM:H₂O) and the extracted product was purified by column chromatography on silica gel with mixtures of hexane and ethyl acetate, as eluents. The product was isolated as a white powder (320 mg, 92%). ¹H-NMR (250 MHz, CDCl₃): δ 5.1 (*s*, 2H, H_d), 7.1 (*d*, JH_eH_f=7.5 Hz, 2H, H_e), 7.3-7.4 (*m*, 5H, H_c, H_b, H_a), 7.8 (*d*, JH_iH_e=7.5 Hz, 2H, H_i), 9.9 (*s*, 1H, H_g) ppm. MS (MALDI-TOF, positive mode): *m/z* 211, [M+H]⁺. Calculated: C₁₄H₁₂O₂: 212.

Synthesis and characterization of the model monoradical (3). In short, the synthesis of compound **3** consisted in the coupling of the aldehyde group of compound **2** with the PTM phosphonate (**1**), followed by the oxidation to the radical with AgNO₃. 397 mg of diethyl-4-[bis(2,3,4,5,6-pentachlorophenyl)methyl]-2,3,5,6-tetrachlorobenzyl phosphonate (452 μmol, 1.2 eq) and 110 mg (980 μmol, 2.6 eq) of potassium tert-butoxide were dissolved in 3 ml of THF. The mixture was stirred for 10 minutes, and a solution of 80 mg of **2** (377 μmol, 1 eq) in 2 ml of THF, was added drop by drop, with a cannula. The reaction mixture changed its color from orange to violet. The reaction was followed up by IR-ATR and NMR and took 18 hours to be complete. Finally, 89 mg of AgNO₃ (452 μmol, 1.2 eq) were added to the reaction mixture and the conversion of the anion into the radical was monitored by UV-Vis. After 2 minutes, an additional 94 mg of AgNO₃ (560 μmol, 1.5 eq) were added. Once the anion was fully converted into radical, the reaction mixture was purified by an aqueous work-up followed by a column chromatography on silica gel with mixtures of hexane and ethyl acetate as eluents. The product was isolated as a brown-green powder (275 mg, 78%). IR-ATR (ν/cm⁻¹): 1600, 1508, 1321, 1244, 1226, 1171, 1016, 965, 948, 815. MS (MALDI-TOF, negative mode): *m/z* 933 [M-H]⁻. Calculated: C₃₄H₁₃Cl₁₄O: 934. EPR (DCM/Toluene 1/1): *g* = 2.0031, *a*_{H1} = 1.9 G, *a*¹³C_α = 29.3 G; *a*¹³C_{arom} = 10.2, 12.5 G; Δ*H*_{pp} = 1.0 G, Δ*H*_{sp} = 3.1 G.

ASSOCIATED CONTENT

Supporting Information

H labels for ¹H NMR spectra assignment, improvements in the PPH-G'n dendrimers synthesis, synthesis of PTM-phosphonate, experimental NMR spectra, MALDI-TOF mass spectra, regression line of the EPR intensity versus the number of radicals plot, EPR spectra with the ¹³C levels, EPR quartet spectra of radical dendrimers, fluorescence microscope images of G₁(PTM*)₁₂ with different fluorescence filters, optical response for each consecutive switching cycle of radical dendrimers, colors of the radical and anion states of the switch of each generation. This material is available free of charge via the internet at <http://pubs.acs.org>.

AUTHOR INFORMATION

Corresponding Author

[*j.vidal@icmab.es](mailto:j.vidal@icmab.es)

Notes

The authors declare no competing financial interests.

ACKNOWLEDGMENT

This work was supported by DGICT-MINECO (MAT2016-80826-R and CTQ2017-90596-REDT), AGAUR (2017 SGR 918), Intramural CSIC project (201760Eo80) and Severo Ochoa FUNMAT-FIP-2018. ICMAB acknowledges Spanish MINECO through the Severo Ochoa Centres of Excellence Programme Grant SEV- 2015-0496.

REFERENCES

- (1) Kitai, J.-i.; Kobayashi, T.; Uchida, W.; Hatakeyama, M.; Yokojima, S.; Nakamura, S.; Uchida, K. Photochromism of a Diarylethene Having an Azulene Ring. *J. Org. Chem.* **2012**, *77*, 3270-3276.
- (2) Métivier, R.; Badré, S.; Méallet-Renault, R.; Yu, P.; Pansu, R. B.; Nakatani, K. Fluorescence Photoswitching in Polymer Matrix: Mutual Influence between Photochromic and Fluorescent Molecules by Energy Transfer Processes. *J. Phys. Chem. C* **2009**, *113*, 11916-11926.
- (3) Feringa, B. L.; van Delden, R. A.; Koumura, N.; Geertsema, E. M. Chiroptical Molecular Switches. *Chem. Rev.* **2000**, *100*, 1789-1816.
- (4) Wang, Y.; Frascioni, M.; Stoddart, J. F. Introducing Stable Radicals into Molecular Machines. *ACS Cent. Sci.* **2017**, *3*, 927-935.
- (5) David, B.; Rafal, K. Integrating Macromolecules with Molecular Switches. *Macromol. Rapid Commun.* **2018**, *39*, 1700827.
- (6) Svenson, S.; Tomalia, D. A. Dendrimers in Biomedical Applications-Reflections on the Field. *Adv. Drug Delivery Rev.* **2005**, *57*, 2106-2129.
- (7) Heegaard, P. M. H.; Boas, U.; Sorensen, N. S. Dendrimers for Vaccine and Immunostimulatory Uses. A Review. *Bioconjug. Chem.* **2010**, *21*, 405-418.
- (8) Boas, U.; Christensen, J. B.; Heegaard, P. M. H. In *Dendrimers in medicine and biotechnology: new molecular tools*; Royal Society of Chemistry: Cambridge, UK, 2006.
- (9) Li, Y.; He, H.; Lu, W.; Jia, X. A Poly(amidoamine) Dendrimer-Based Drug Carrier for Delivering DOX to Gliomas Cells. *RSC Advances* **2017**, *7*, 15475-15481.
- (10) Martiniano, B.; Jonathan, F.-V.; José, C.-B. Theoretical Studies for Dendrimer-Based Drug Delivery. *Curr. Pharm. Des.* **2017**, *23*, 3048-3061.
- (11) Liko, F.; Hindré, F.; Fernandez-Megia, E. Dendrimers as Innovative Radiopharmaceuticals in Cancer Radionanotherapy. *Biomacromolecules* **2016**, *17*, 3103-3114.
- (12) Lei, X.-g.; Jockusch, S.; Turro, N. J.; Tomalia, D. A.; Ottaviani, M. F. J. EPR Characterization of Gadolinium(III)-Containing-PAMAM-Dendrimers in the Absence and in the Presence of Paramagnetic Probes. *Colloid Interface Sci.* **2008**, *322*, 457-464.
- (13) Francese, G.; Dunand, F. A.; Loosli, C.; Merbach, A. E.; Decurtins, S. Functionalization of PAMAM Dendrimers with Nitronyl Nitroxide Radicals as Models for the Outer-Sphere Relaxation in Dentritic Potential MRI Contrast Agents. *Magn. Reson. Chem.* **2003**, *41*, 81-83.
- (14) Han, H. J.; Sebby, K. B.; Singel, D. J.; Cloninger, M. J. EPR Characterization of Heterogeneously Functionalized Dendrimers. *Macromolecules* **2007**, *40*, 3030-3033.
- (15) Badetti, E.; Lloveras, V.; Wurst, K.; Sebastián, R. M.; Caminade, A.-M.; Majoral, J.-P.; Veciana, J.; Vidal-Gancedo, J. Synthesis and Structural Characterization of a Dendrimer Model Compound Based on a Cyclotriphosphazene Core with TEMPO Radicals as Substituents. *Org. Lett.* **2013**, *15*, 3490-3493.
- (16) Badetti, E.; Lloveras, V.; Muñoz-Gómez, J. L.; Sebastián, R. M. a.; Caminade, A. M.; Majoral, J. P.; Veciana, J.; Vidal-Gancedo, J. Radical Dendrimers: A Family of Five Generations of Phosphorus Dendrimers Functionalized with TEMPO Radicals. *Macromolecules* **2014**, *47*, 7717-7724.
- (17) Lloveras, V.; Liko, F.; Pinto, L. F.; Muñoz-Gómez, J. L.; Veciana, J.; Vidal-Gancedo, J. Tuning Spin-Spin Interactions in Radical Dendrimers. *ChemPhysChem* **2018**, *19*, 1895-1902.
- (18) Kannan, R. M.; Nance, E.; Kannan, S.; Tomalia, D. A. Emerging Concepts in Dendrimer-Based Nanomedicine: from Design Principles to Clinical Applications. *J. Intern. Med.* **2014**, *276*, 579-617.
- (19) Mintzer, M. A.; Grinstaff, M. W. Biomedical applications of dendrimers: a tutorial. *Chem. Soc. Rev.* **2011**, *40*, 173-190.
- (20) Astruc, D. Electron-Transfer Processes in Dendrimers and their Implication in Biology, Catalysis, Sensing and Nanotechnology. *Nature Chem.* **2012**, *4*, 255-257.
- (21) Rajca, A. Organic Diradicals and Polyradicals: From Spin Coupling to Magnetism? *Chem. Rev.* **1994**, *94*, 871-893.
- (22) Turrin, C.-O.; Chiffre, J.; de Montauzon, D.; Balavoine, G.; Manoury, E.; Caminade, A.-M.; Majoral, J.-P. Behavior of an Optically Active Ferrocene Chiral Shell Located within Phosphorus-Containing Dendrimers. *Organometallics* **2002**, *21*, 1891-1897.
- (23) Alonso, B.; Moran, M.; Casado, C. M.; Lobete, F.; Losada, J.; Cuadrado, I. Electrodes Modified with Electroactive Films of Organometallic Dendrimers. *Chem. Mater.* **1995**, *7*, 1440-1442.
- (24) Ganesamoorthy, R.; Sathiyam, G.; Sakthivel, P. Review: Fullerene Based Acceptors for Efficient Bulk Heterojunction Organic Solar Cell Applications. *Sol. Energy Mater. Sol. Cells* **2017**, *161*, 102-148.
- (25) Long, D.-L.; Burkholder, E.; Cronin, L. Polyoxometalate Clusters, Nanostructures and Materials: From Self Assembly to Designer Materials and Devices. *Chem. Soc. Rev.* **2007**, *36*, 105-121.
- (26) Buades, A. B.; Arderiu, V. S.; Olid-Britos, D.; Viñas, C.; Sillanpää, R.; Haukka, M.; Fontrodona, X.; Paradinas, M.; Ocal, C.; Teixidor, F. Electron Accumulative Molecules. *J. Am. Chem. Soc.* **2018**, *140*, 2957-2970.
- (27) Djeda, R.; Ornelas, C.; Ruiz, J.; Astruc, D. Branching the Electron-Reservoir Complex [Fe(η^5 -C₅H₅)(η^6 -C₆Me₆)]PF₆ onto Large Dendrimers: "Click", Amide, and Ionic Bonds. *Inorg. Chem.* **2010**, *49*, 6085-6101.
- (28) Lloveras, V.; Badetti, E.; Chechik, V.; Vidal-Gancedo, J. Magnetic Interactions in Spin-Labeled Au Nanoparticles. *J. Phys. Chem. C* **2014**, *118*, 21622-21629.
- (29) Lloveras, V.; Badetti, E.; Wurst, K.; Chechik, V.; Veciana, J.; Vidal-Gancedo, J. Magnetic and Electrochemical Properties of a TEMPO-Substituted Disulfide Diradical in Solution, in the Crystal, and on a Surface. *Chem. Eur. J.* **2016**, *22*, 1805-1815.
- (30) Lloveras, V.; Badetti, E.; Veciana, J.; Vidal-Gancedo, J. Dynamics of Intramolecular Spin Exchange Interaction of a Nitronyl Nitroxide Diradical in Solution and on Surfaces. *Nanoscale* **2016**, *8*, 5049-5058.
- (31) Pinto, L.F.; Marín-Montesinos, I.; Lloveras, V.; Muñoz-Gómez, J.L.; Pons, M.; Veciana, J.; Vidal-Gancedo, J. NMR Signal Enhancement > 50000 times in Fast Dissolution Dynamic Nuclear Polarization. *Chem. Commun.* **2017**, *53*, 3757-3760.
- (32) Ballester, M.; Riera-Figueras, J.; Castaner, J.; Badfa, C.; Monso, J. M. Inert Carbon Free Radicals. I. Perchlorodiphenylmethyl and Perchlorotriphenylmethyl Radical Series. *J. Am. Chem. Soc.* **1971**, *93*, 2215-2225.
- (33) Launay, N.; Caminade, A.-M.; Majoral, J. P. Synthesis of Bowl-Shaped Dendrimers From Generation 1 to Generation 8. *J. Organomet. Chem.* **1997**, *529*, 51-58.
- (34) Rovira, C.; Ruiz-Molina, D.; Elsner, O.; Vidal-Gancedo, J.; Bonvoisin, J.; Launay, J.-P.; Veciana, J. Influence of Topology on the Long-Range Electron-Transfer Phenomenon. *Chem. Eur. J.* **2001**, *7*, 240-250.
- (35) Prévôté, D.; Le Roy-Gourvenec, S.; Caminade, A. M.; Masson, S.; Majoral, J. P. Application of the Horner-Wadsworth-Emmons Reaction to the Functionalization of Dendrimers: Synthesis of Amino Acid Terminated Dendrimers. *Synthesis* **1997**, *1997*, 1199-1207.
- (36) Franco, C.; Mas-Torrent, M.; Caballero, A.; Espinosa, A.; Molina, P.; Veciana, J.; Rovira, C. Pyrene-based dyad and triad leading to a reversible chemical and redox optical and magnetic switch. *Chem. Eur. J.* **2015**, *21*, 5504-5509.
- (37) Frisenda, R.; Gaudenzi, R.; Franco, C.; Mas-Torrent, M.; Rovira, C.; Veciana, J.; Alcon, I.; Bromley, S. T.; Burzurí, E.; Van Der Zant, H. S. J. Kondo Effect in a Neutral and Stable All Organic Radical Single Molecule Break Junction. *Nano Lett.* **2015**, *15*, 3109-3114.

(38) Yuan, L.; Franco, C.; Crivillers, N.; Mas-Torrent, M.; Sangeeth, C. S. S.; Rovira, C.; Veciana, J.; Nijhuis, C. A. Chemical control over the energy level alignment in a two-terminal junction. *Nat. Commun.* **2016**, *7*, 12066-12076.

(39) Franco, C.; Mayorga Burrezo, P.; Lloveras, V.; Caballero, R.; Alcón, I.; Bromley, S. T.; Mas-Torrent, M.; Langa, F.; López Navarrete, J. T.; Rovira, C.; Casado, J.; Veciana, J. Operative Mechanism of Hole-Assisted Negative Charge Motion in Ground States of Radical-Anion Molecular Wires. *J. Am. Chem. Soc.* **2017**, *139*, 686-692.

(40) Badetti, E.; Caminade, A.-M.; Majoral, J.-P.; Moreno-Mañas, M.; Sebastián, R. M. Palladium(0) Nanoparticles Stabilized by Phosphorus Dendrimers Containing Coordinating 15-Membered Triolefinic Macrocycles in Periphery. *Langmuir* **2008**, *24*, 2090-2101.

(41) Blais, J.-C.; Turrin, C.-O.; Caminade, A.-M.; Majoral, J.-P. MALDI TOF Mass Spectrometry for the Characterization of Phosphorus-Containing Dendrimers. Scope and Limitations. *Anal. Chem.* **2000**, *72*, 5097-5105.

(42) Armet, O.; Veciana, J.; Rovira, C.; Riera, J.; Castaner, J.; Molins, E.; Rius, J.; Miravittles, C.; Olivella, S.; Brichfeus, J. Inert Carbon Free Radicals. 8. Polychlorotriphenylmethyl Radicals: Synthesis, Structure, and Spin-Density Distribution. *J. Phys. Chem.* **1987**, *91*, 5608-5616.

(43) McGlynn, S.; Azumi, T.; Kinoshita, M. In *Molecular spectroscopy of the triplet state* / S. P. McGlynn, T. Azumi, M. Kinoshita; Prentice-Hall: Englewood Cliffs, NJ, 1969.

(44) Eaton, S. S.; More, K. M.; Sawant, B. M.; Eaton, G. R. Use of the ESR Half-Field Transition to Determine the Interspin Distance and the Orientation of the Interspin Vector in Systems with Two Unpaired Electrons. *J. Am. Chem. Soc.* **1983**, *105*, 6560-6567.

(45) Crivillers, N.; Mas-Torrent, M.; Vidal-Gancedo, J.; Veciana, J.; Rovira, C. Self-Assembled Monolayers of Electroactive Polychlorotriphenylmethyl Radicals on Au(111). *J. Am. Chem. Soc.* **2008**, *130*, 5499-5506.

(46) Lloveras, V.; Vidal-Gancedo, J.; Figueira-Duarte, T. M.; Nierengarten, J.-F.; Novoa, J. J.; Mota, F.; Ventosa, N.; Rovira, C.; Veciana, J. Tunneling Versus Hopping in Mixed-Valence Oligo-p-Phenylenevinylene Polychlorinated Bis(triphenylmethyl) Radical Anions. *J. Am. Chem. Soc.* **2011**, *133*, 5818-5833.

(47) Veciana, J.; Rovira, C.; Ventosa, N.; Crespo, M. I.; Palacio, F. Stable Polyradicals with High-Spin Ground States. 2. Synthesis and Characterization of a Complete Series of Polyradicals Derived from 2,4,6-trichloro- α,α,α' -hexakis(pentachlorophenyl)mesitylene with $S = 1/2, 1$, and $3/2$ Ground States. *J. Am. Chem. Soc.* **1993**, *115*, 57-64.

TOC

Manuscript ID: cm-2019-03015j

